Signal-to-noise ratio trade-offs associated with coarsely sampled Fourier transform spectroscopy

Samuel T. Thurman* and James R. Fienup

The Institute of Optics, University of Rochester, Rochester, New York 14627
**Corresponding author: thurman@optics.rochester.edu*

Received March 5, 2007; accepted April 26, 2007;
posted May 31, 2007 (Doc. ID 80630); published August 9, 2007

We derive the spectral signal-to-noise ratio (SNR) trade-offs associated with coarsely sampled Fourier transform spectroscopy using a step-and-integrate measurement scheme. We show that there is no SNR penalty in the shot noise limit and a slight SNR benefit in the detector noise limit for the case of coarse sampling to achieve the same spectral resolution as a baseline Nyquist sampling scenario, where the total detector integration time is the same for both sampling cases. © 2007 Optical Society of America

OCIS codes: 300.6300, 070.6020.

1. INTRODUCTION

The Nyquist sampling criterion [1,2] states that a band-limited signal $f(\tau)$ can be completely specified by an infinite set of uniformly spaced samples, provided that the sample spacing $\Delta\tau$ satisfies the Nyquist sampling condition $\Delta\tau \leqslant 1/(2\nu_{\max})$, where $F(\nu)$, the Fourier transform of $f(\tau)$, vanishes for $|\nu| > \nu_{\max}$. In some cases, e.g., if $f(\tau)$ has a one-sided or bandpass spectrum, it is possible to use a coarser sample spacing and yet completely specify $f(\tau)$ [3].

We consider the signal-to-noise (SNR) trade-offs associated with coarse sampling [4–8] for Fourier transform spectroscopy (FTS) using the step-and-integrate method of data collection [7,8]. For the case of an ideal Michelson-interferometer-based instrument, the response, $h(\tau)$, of a detector at the output plane of the interferometer varies with the time delay, τ, between the arms of the interferometer as [9]

$$h(\tau) = \frac{t_d}{2}\int_0^\infty S(\nu)[1+\cos(2\pi\nu\tau)]\mathrm{d}\nu, \tag{1}$$

where t_d is the detector integration time per measurement, $S(\nu)$ is the spectrum of the source as seen by the detector in units of photoelectrons/s/Hz, and the optical path difference (OPD) between the arms of the interferometer is given by $c\tau$ with c being the speed of light. The modulation of the interference pattern is given by

$$f(\tau) = h(\tau) - \bar{h} = \frac{t_d}{2}\int_0^\infty S(\nu)\cos(2\pi\nu\tau)\mathrm{d}\nu, \tag{2}$$

where $\bar{h}$ is the average of $h(\tau)$ over all τ, i.e.,

$$\bar{h} = \frac{t_d}{2}\int_0^\infty S(\nu)\mathrm{d}\nu. \tag{3}$$

The continuous Fourier transform of $f(\tau)$ is given by

$$F(\nu) = \int_{-\infty}^{\infty} f(\tau)\exp(-i2\pi\nu\tau)\mathrm{d}\tau = \frac{t_d}{4}[S(\nu)+S(-\nu)]. \tag{4}$$

In practice, only a finite number, N, of measurement samples can be made, say,

$$g_n = f(n\Delta\tau), \tag{5}$$

where the subscript $n \in \{-N/2, -N/2+1, \ldots, (N-2)/2\}$, for even N, is an integer sample index and $\Delta\tau$ is the sample spacing. Thus, spectral information is obtained via the discrete Fourier transform (DFT), defined as

$$G_p = \frac{1}{\sqrt{N}}\sum_{n=-N/2}^{N/2-1} g_n \exp\left(-i2\pi\frac{np}{N}\right), \tag{6}$$

for $p \in \{-N/2, -N/2+1, \ldots, (N-2)/2\}$. The DFT samples G_p can be expressed in terms of the continuous Fourier transform $F(\nu)$ as (see Appendix A)

$$G_p = \frac{1}{\sqrt{N}\Delta\tau}\int_{-\infty}^{\infty}\left\{F(\nu)\otimes\left[\frac{1}{\Delta\nu}\mathrm{sinc}\left(\frac{\nu}{\Delta\nu}\right)\right]\otimes\left[\frac{1}{N\Delta\nu}\mathrm{comb}\left(\frac{\nu}{N\Delta\nu}\right)\right]\right\}\delta(\nu-p\Delta\nu)\mathrm{d}\nu, \tag{7}$$

where the $\otimes$ symbol represents a convolution operation, $\mathrm{sinc}(x) = \sin(\pi x)/(\pi x)$, $\mathrm{comb}(x) = \sum_{k=-\infty}^{\infty}\delta(x-k)$, $\delta(x)$ is the Dirac delta function, and

$$\Delta\nu = 1/(N\Delta\tau) \tag{8}$$

is the spectral sampling interval. The primary effect of the sinc convolution is to limit the full width at half-maximum spectral resolution of G_p to $1.21\Delta\nu$ (or peak-to-first-null resolution of $\Delta\nu$). We will ignore the sinc convolution for notational convenience and rewrite Eq. (7) as

 © 2007 Optical Society of America

$$G_p = \frac{1}{\sqrt{N}\Delta\tau}\int_{-\infty}^{\infty} F(\nu)\frac{1}{N\Delta\nu}\mathrm{comb}\left(\frac{\nu - p\Delta\nu}{N\Delta\nu}\right)\mathrm{d}\nu$$

$$= \frac{t_d}{4\sqrt{N}\Delta\tau}\sum_{q=-\infty}^{\infty} S[(p-qN)\Delta\nu] + S[-(p-qN)\Delta\nu], \quad (9)$$

where the sinc convolution is now embedded in $S(\nu)$. The effect of the comb convolution is to sum periodically shifted copies of $S(\nu)$ with a period equal to $N\Delta\nu$, thus "aliasing" high frequency ($|\nu| \geqslant N\Delta\nu/2$) information into the interval over which G_p is defined ($|\nu| \leqslant N\Delta\nu/2$). Aliasing can be problematic if the nonzero portions of each shifted copy of $S(\nu)$ overlap. The Nyquist sampling condition ensures that this does not occur for $f(\tau)$ bandlimited to $|\nu| \leqslant \nu_{\max}$. However, in cases where $S(\nu)$ is a bandpass spectrum, it may be possible to use a coarser τ-domain sampling and still ensure that the nonzero portions of each shifted copy of $S(\nu)$ do not overlap. In such cases, high-spatial-frequency information can be dealiased using *a priori* knowledge of the bandpass interval of $S(\nu)$.

Coarse sampling is a well-known technique [4–8] and has several advantages over Nyquist sampling related to the fact that coarse sampling can obtain the same spectral resolution as Nyquist sampling, but with fewer measurements. In imaging FTS, where raw data sets can be very large and even problematic, coarse sampling by a factor of 2–4 can provide some data reduction. Also, making fewer measurements within the same data collection time reduces the data rate, enabling the use of slower readout and recording electronics (although the readout process cannot be lengthened arbitrarily). Coarse sampling requires fewer mechanical stepping motions during data collection, which can be easier on hardware. If SNR is not an issue, coarse sampling can be used to reduce the total data collection time [7,8]. However, SNR is often one of the most important issues. In Section 2 we derive the spectral SNR for coarsely sampled FTS. Section 3 analyzes the SNR trade-offs of coarse sampling in comparison with Nyquist sampling for the detector and shot noise limits. We show that there is no SNR penalty in the shot noise limit and there is a slight SNR advantage in the detector noise limit for coarse sampling to achieve the same spectral sampling/resolution as a Nyquist sampling case, for the same total detector integration time in both sampling cases. Section 4 contains a coarsely sampled FTS example. Section 5 is a summary.

2. SPECTRAL SNR

In addition to g_n, each measurement sample includes noise ε_n. We consider the case of zero-mean, statistically independent noise where the noise covariance is given by

$$\langle \varepsilon_m \varepsilon_n \rangle = \sigma_{\tau,n}^2 \delta_{m,n}, \quad (10)$$

where $\delta_{m,n}$ is the Kronecker delta function,

$$\sigma_{\tau,n}^2 = \sigma_d^2 + h(n\Delta\tau), \quad (11)$$

and σ_d^2 is the variance of the detector noise and the second term is the variance of the shot noise associated with the intensity of the interference pattern $h(\tau)$ given in units of detected photoelectrons. Since the visibility of the interference pattern tends to be small for large OPDs between the arms of the interferometer, the following approximation is typically valid:

$$\sigma_{\tau,n}^2 \approx \sigma_d^2 + \bar{h} = \sigma_d^2 + \frac{t_d}{2}\int_0^{\infty} S(\nu)\mathrm{d}\nu. \quad (12)$$

Assuming that the noise in each sample is independent, the variance of the real part of the DFT of the noise in computing G_p is given by

$$\sigma_{\nu,p}^2 = \left\langle \left[\frac{1}{\sqrt{N}} \sum_{n=-N/2}^{N/2} \varepsilon_n \cos\left(-i2\pi\frac{pn}{N}\right)\right]^2 \right\rangle$$

$$= \frac{1}{N}\sum_{m=-N/2}^{N/2}\sum_{n=-N/2}^{N/2} \langle \varepsilon_m \varepsilon_n \rangle \cos\left(-2\pi\frac{pm}{N}\right)\cos\left(-2\pi\frac{pn}{N}\right),$$

$$= \frac{1}{N}\sum_{n=-N/2}^{N/2} \sigma_{\tau,n}^2 \cos^2\left(2\pi\frac{pn}{N}\right), \quad (13)$$

where we have made use of Eq. (10). Substituting Eq. (12) into this expression and simplifying yields

$$\sigma_{\nu,p}^2 = \left[\frac{\sigma_d^2}{2} + \frac{t_d}{4}\int_0^{\infty} S(\nu)\mathrm{d}\nu\right](1 + \delta_{p,0} + \delta_{p,-N/2}). \quad (14)$$

The spectral SNR is defined as the ratio of the spectral signal, G_p, to the standard deviation of the noise in that signal, $\sigma_{\nu,p}$, i.e.,

$$SNR_p = \frac{G_p}{\sigma_{\nu,p}}. \quad (15)$$

A. Detector Noise Limit

When detector noise dominates, i.e.,

$$\sigma_d^2 \gg \frac{t_d}{2}\int_0^{\infty} S(\nu)\mathrm{d}\nu, \quad (16)$$

the spectral SNR can be approximated as

$$SNR_{d,p} = \frac{t_d \sum_{q=-\infty}^{\infty} S[(p-qN)\Delta\nu] + S[-(p-qN)\Delta\nu]}{2\sqrt{2N}\sigma_d\Delta\tau\sqrt{(1 + \delta_{p,0} + \delta_{p,-N/2})}}, \quad (17)$$

where typically only one of the terms in the infinite sum will be nonzero for any given p. Thus, $SNR_{d,p}$ obeys the following proportionality relation:

$$SNR_{d,p} \propto \frac{t_d}{\sqrt{N}\Delta\tau} = \sqrt{N} t_d \Delta\nu. \quad (18)$$

B. Shot Noise Limit

When shot noise dominates, i.e.,

$$\frac{t_d}{2}\int_0^{\infty} S(\nu)\mathrm{d}\nu \gg \sigma_d^2, \quad (19)$$

the spectral SNR can be approximated as

$$SNR_{s,p} = \frac{\sqrt{t_d}\sum_{q=-\infty}^{\infty} S[(p-qN)\Delta\nu] + S[-(p-qN)\Delta\nu]}{2\sqrt{N}\Delta\tau\sqrt{\int_0^\infty S(\nu)\mathrm{d}\nu(1+\delta_{p,0}+\delta_{p,-N/2})}}, \tag{20}$$

which scales as

$$SNR_{s,p} \propto \frac{\sqrt{t_d}}{\sqrt{N}\Delta\tau} = \sqrt{Nt_d}\Delta\nu. \tag{21}$$

3. TRADE-OFFS

Consider the ideal scenario in which there is no temporal overhead associated with each measurement, such that the detector integration time for each g_n sample is given by

$$t_d = T/N, \tag{22}$$

where T is the time for making all N measurements. Tables 1 and 2 list the trade-offs associated with coarse sampling in comparison with Nyquist sampling for three specific cases of coarse sampling with a constant T: (i) coarse sampling using the same number of samples as the Nyquist sampling case, but sampling over a wider range of OPDs to achieve finer spectral resolution; (ii) coarse sampling to yield the same spectral sampling as the Nyquist sampling case, but with fewer OPD samples; and (iii) coarse sampling to yield the same spectral SNR as the Nyquist sampling case, but with fewer OPD samples while holding constant the spectral SNR given by either Eq. (17) or Eq. (20). In the tables, $\Delta\tau_0$ and N_0 represent the sample spacing and number of samples used for the Nyquist sampling case, respectively. For each case, the integration time t_d is calculated using Eq. (21), the spectral sampling $\Delta\nu$ is calculated using Eq. (8), and the spectral SNR is calculated using either Eq. (17) or Eq. (20). The degree of coarse sampling, represented by the factor α, is greater than unity for coarse sampling and less than unity for oversampling. From Table 1 we see that coarse sampling in the detector noise limit with N_0 samples yields a spectral sampling/resolution, $\Delta\nu$ that is improved by a factor of $1/\alpha$ and a spectral SNR that is reduced by a factor of $1/\alpha$ in comparison with Nyquist sampling; coarse sampling with N_0/α samples yields the same $\Delta\nu$ but a SNR that is increased by $\sqrt{\alpha}$ compared with Nyquist sampling; coarse sampling with $\alpha^{-2/3}N_0$ samples yields a $\Delta\nu$ that is improved by $\alpha^{-1/3}$ with the same SNR as Nyquist sampling. From Table 2, we see that the coarse sampling in the shot noise limit with N_0 samples yields the same trade-offs as in the detector noise limit; i.e., $\Delta\nu$ and the spectral SNR are reduced by $1/\alpha$ compared with Nyquist sampling, which results from the fact that SNR_d and SNR_s scale identically with $\Delta\tau$, as indicated by Eqs. (17) and (20). Note that the last two columns of Table 2 are identical, i.e., coarse sampling with N_0/α samples in the shot noise limit yields the same $\Delta\nu$ and spectral SNR as the Nyquist sampling case, and differ from the detector-noise-limited case.

In practice there usually is some temporal overhead associated with making each measurement. For example, stepping the time delay between measurements typically requires the physical movement of a mirror or corner cube in the interferometer and waiting for vibrations to settle, and the time to read out a large detector array in the case of imaging FTS may be nonnegligible. Assuming that the temporal overhead, t_s, associated with stepping the time delay between each successive measurement is fixed, t_d is given by the following equation instead of Eq. (21):

$$t_d = \frac{T - Nt_s}{N}. \tag{23}$$

Thus, coarse sampling with a smaller N has the benefit of using a larger fraction of the total time T for detector integration.

4. EXAMPLE

To illustrate coarsely sampled FTS and the SNR trade-offs, we simulate the measurement of the American Society for Testing and Materials reference solar spectrum [10] over the ν=118.3–157.8 THz (λ=1.900–2.535 μm) spectral band. For the simulation, $S(\nu)$ was the bandlimited ASTM G173-03 spectrum converted to photoelectron

Table 1. Coarse versus Nyquist Sampling Trade-Offs in the Detector Noise Limit

		Coarse Sampling		
	Nyquist Sampling	Same Number of Samples, N	Same Spectral Sampling, $\Delta\nu$	Same Spectral SNR
Sample Spacing, $\Delta\tau$	$\Delta\tau_0$	$\alpha\Delta\tau_0$	$\alpha\Delta\tau_0$	$\alpha\Delta\tau_0$
Number of Samples, N	N_0	N_0	$\frac{N_0}{\alpha}$	$\frac{N_0}{\alpha^{2/3}}$
Intergration Time, t_d	t_0	t_0	αt_0	$\alpha^{2/3}t_0$
Spectral Sampling, $\Delta\nu$	$\Delta\nu_0$	$\frac{\Delta\nu_0}{\alpha}$	$\Delta\nu_0$	$\frac{\Delta\nu_0}{\alpha^{1/3}}$
Spectral SNR	SNR_0	$\frac{SNR_0}{\alpha}$	$\sqrt{\alpha}SNR_0$	SNR_0

Table 2. Coarse versus Nyquist Sampling Trade-Offs in the Shot Noise Limit

		Coarse Sampling		
	Nyquist Sampling	Same Number of Samples, N	Same Spectral Sampling, $\Delta\nu$	Same Spectral SNR
Sample Spacing, $\Delta\tau$	$\Delta\tau_0$	$\alpha\Delta\tau_0$	$\alpha\Delta\tau_0$	$\alpha\Delta\tau_0$
Number of Samples, N	N_0	N_0	$\frac{N_0}{\alpha}$	$\frac{N_0}{\alpha}$
Integration Time, t_d	t_0	t_0	$\alpha\tau_0$	$\alpha\tau_0$
Spectral Sampling, $\Delta\nu$	$\Delta\nu_0$	$\frac{\Delta\nu_0}{\alpha}$	$\Delta\nu_0$	$\Delta\nu_0$
Spectral SNR	SNR_0	$\frac{SNR_0}{\alpha}$	SNR_0	SNR_0

units and scaled to have an integrated flux of 10^7 photoelectrons/s as seen by a detector with a uniform spectral response. Figure 1(a) shows a spectrum calculated from a noiseless set of Nyquist sampled ($\alpha=1$) intensity samples for $N_0=384$, a total integration time of $T=1$ s, and $t_s=0$ s. Figure 1(b) shows a noisy spectrum calculated from the same set of Nyquist samples plus Poisson shot noise and Gaussian detector noise with a σ_d

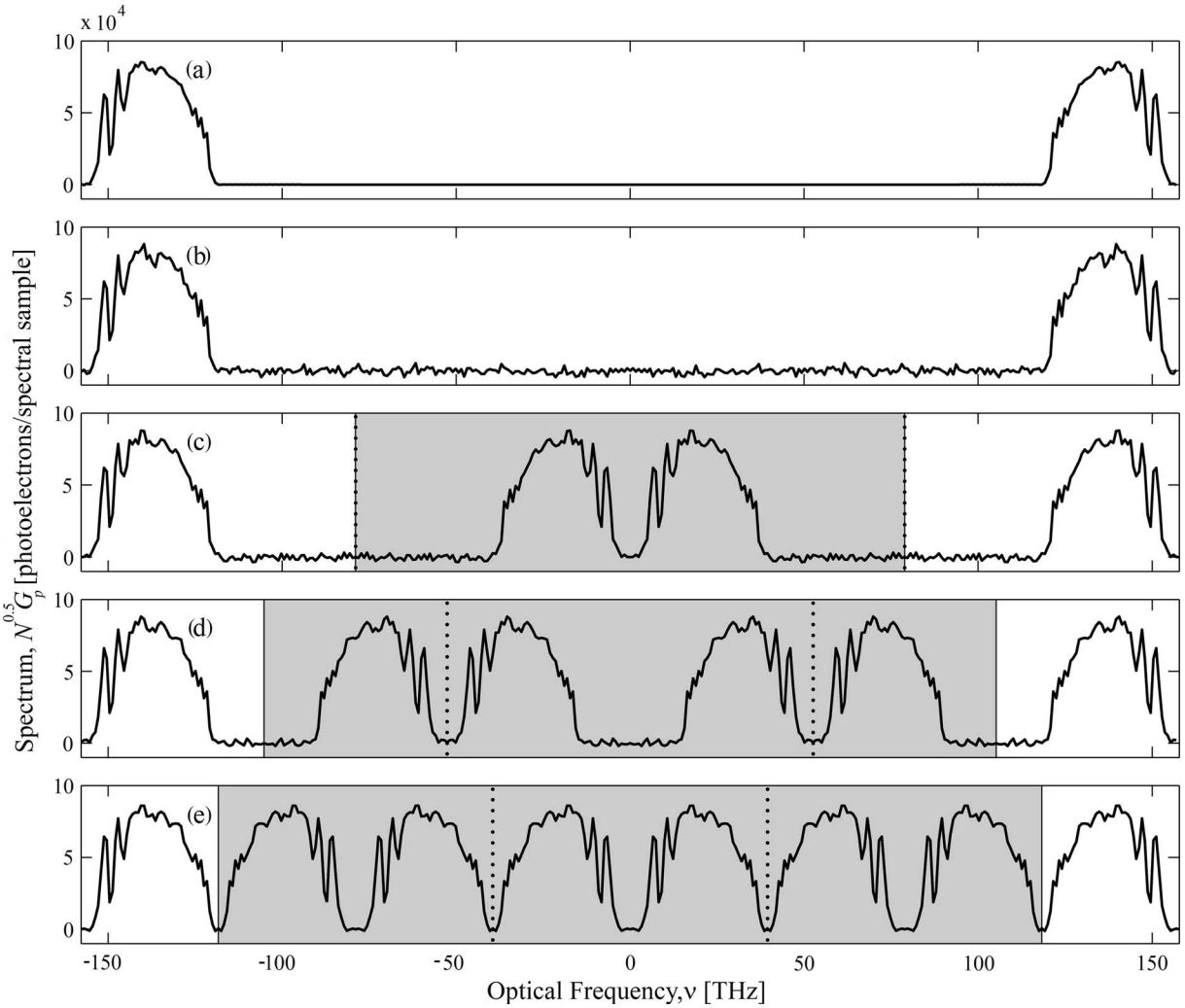

Fig. 1. Example spectra recovered from simulated FTS measurements (a) without noise, (b) with detector and shot noise, and (c)–(e) additionally with undersampling. For (a) and (b) $\alpha=1$ (Nyquist sampling), $N=384$; for (c) $\alpha=2$, $N=192$; for (d) $\alpha=3$, $N=128$; and for (e) $\alpha=4$, $N=96$. For the coarse sampling cases ($\alpha>1$), the unshaded regions indicate the extent of unaliased spectra, while the shaded regions contain aliased spectra. The vertical dotted lines in (c)–(e) indicate the extent of each length N DFT of the coarsely sampled data.

=70 photoelectrons. The measurements are dominated by shot noise since

$$\frac{t_0}{2}\int_0^\infty S(\nu)\mathrm{d}\nu = 1.3\times 10^4 \text{ photoelectrons} \tag{24}$$

is greater than σ_d^2 for the Nyquist sampling case and the shot noise only increases for the coarse sampling cases. Figures 1(c)–1(e) show noisy spectra obtained from coarsely sampled intensity measurements for $\alpha=2$, 3, and 4 with $N=N_0/\alpha$ samples (such that each spectrum in Fig. 1 has the same spectral sampling/resolution). Aliased spectra obtained from the coarse FTS measurements are in the shaded regions of Figs. 1(c)–1(e), while unaliased spectra are in the unshaded regions. In each case, the unaliased spectrum is constructed by simply bandlimiting the periodically extended spectrum to the *a priori* known spectral bandwidth of $S(\nu)$. Referring to Table 2, the spectral SNR is independent of α in the shot noise limit, with coarse sampling to obtain a fixed $\Delta\nu$. The root-mean-square errors of the noisy spectra shown in Figs. 1(b)–1(e), calculated with respect to the noiseless spectra shown in Fig. 1(a) over the range $\nu=118.3-157.8$ THz are 1.89×10^3, 1.82×10^3, 1.64×10^3, and 1.76×10^3 [photoelectrons/spectral sample], respectively, which are equivalent to within the statistical fluctuations observed in simulating the data with different noise realizations.

In this example, note that the aliased spectrum is close to the dc frequency, $\nu=0$, when $\alpha=2$ or 4, as shown in Figs. 1(c) and 1(e). While we have not considered it in this analysis, $1/f$ noise or source intensity fluctuations on time scales longer than t_d yield "pink" noise that is concentrated at low ν values. In the presence of such noise sources, coarse sampling such that the aliased spectrum appears close to $\nu=0$ can yield a lower SNR.

5. SUMMARY

We have derived the SNR trade-offs associated with coarse sampling step-and-integrate FTS. These results indicate that for the case of coarse sampling to obtain the same spectral resolution as in a baseline Nyquist sampling scenario, there is no SNR penalty in the shot noise limit and there is a SNR benefit in the detector noise limit. These results assume that the total data collection time is equal for both cases and that there is no temporal overhead associated with making each measurement. These results imply that the additional benefits associated with coarse sampling, such as smaller data sets and fewer stepping motions during data collection, can be had without a loss in SNR.

APPENDIX A

Using the same notation as in the Introduction, we wish to express the DFT G_p in terms of the continuous Fourier transform $F(\nu)$. Using Eqs. (5) and (8), Eq. (6) can be written as

$$G_p = \frac{1}{\sqrt{N}}\sum_{n=-N/2}^{N/2-1}\int_{-\infty}^{\infty}\int_{-\infty}^{\infty} f(\tau)\exp(-i2\pi\nu\tau) \times\delta(\tau-n\Delta\tau)\,\delta(\nu-p\Delta\nu)\mathrm{d}\tau\mathrm{d}\nu. \tag{A1}$$

Moving the summation operator inside the integrals, G_p can be expressed as

$$G_p = \operatorname*{Lim}_{\varepsilon\to0^+}\frac{1}{\sqrt{N}}\int_{-\infty}^{\infty}\int_{-\infty}^{\infty} f(\tau)\,\mathrm{rect}\left(\frac{\tau+\varepsilon}{N\Delta\tau}\right)\left[\frac{1}{\Delta\tau}\mathrm{comb}\left(\frac{\tau}{\Delta\tau}\right)\right] \times\exp(-i2\pi\nu\tau)\,\delta(\nu-p\Delta\nu)\mathrm{d}\tau\mathrm{d}\nu, \tag{A2}$$

where $\mathrm{rect}(x)=1$ for $|x|\leq0.5$ and 0 for $|x|>0.5$. By evaluating the continuous Fourier transform integral and the limit, G_p can be expressed in terms of $F(\nu)$ as

$$G_p = \frac{1}{\sqrt{N}\Delta\tau}\int_{-\infty}^{\infty}\left\{F(\nu)\otimes\left[\frac{1}{\Delta\nu}\mathrm{sinc}\left(\frac{\nu}{\Delta\nu}\right)\right] \otimes\left[\frac{1}{N\Delta\nu}\mathrm{comb}\left(\frac{\nu}{N\Delta\nu}\right)\right]\right\}\delta(\nu-p\Delta\nu)\mathrm{d}\nu. \tag{A3}$$

ACKNOWLEDGMENT

This work was supported by Lockheed Martin Corporation.

REFERENCES

1. H. Nyquist, "Certain topics in telegraph transmission theory," Trans. Am. Inst. Electr. Eng. **47**, 617–644 (1928).
2. E. T. Whittaker, "On the functions which are represented by the expansions of the interpolation theory," Proc. R. Soc. Edinburgh, Sect. A: Math. Phys. Sci. **35**, 181–194 (1915).
3. C. E. Shannon, "Communication in the presence of noise," Proc. Inst. Radio Eng. **37**, 10–21 (1949).
4. J. Connes, "Spectroscopic studies using Fourier transformations," Rev. Opt. Theor. Instrum. **40**, 116 (1961).
5. G. A. Vanasse and H. Sakai, "Fourier spectroscopy," in *Progress in Optics*, Vol. 6, E. Wolf, ed. (North-Holland, 1967), pp. 261–330.
6. J. Kauppinen, "Correction of the linear phase errors of one-sided interferograms," Infrared Phys. **16**, 359–366 (1976).
7. D. A. Naylor, B. G. Gom, M. K. Tahic, and G. R. Davis, "Astronomical spectroscopy using an aliased, step-and-integrate, Fourier transform spectrometer," Proc. SPIE **5498**, 685–694 (2004).
8. D. A. Naylor, B. G. Gom, T. R. Fulton, M. K. Tahic, and G. R. Davis, "Increased efficiency through undersampling in Fourier transform spectroscopy," presented at the OSA Topical Meeting, "Fourier Transform Spectroscopy/Hyperspectral Imaging and Sounding of the Environment," Alexandria, Va., January 31–February 3, 2005.
9. J. Kauppinen and J. Partanen, *Fourier Transforms in Spectroscopy* (Wiley-VCH, 2001).
10. ASTM International, "Standard tables for reference solar spectral irradiances: direct normal and hemispherical on 37° tilted surface," standard G173-03, http://www.astm.org (2003).